Appl Biochem Biotechnol (2009) 158:262–276
DOI 10.1007/s12010-008-8351-8

Breakthrough Model of Recombinant Human-Like Collagen in Immobilized Metal Affinity Chromatography

Xiao-Jun Wang · Dai-Di Fan · Yan-E Luo

Received: 11 May 2008 / Accepted: 18 August 2008 /
Published online: 9 September 2008

Abstract The adsorption of recombinant human-like collagen by metal chelate media was investigated in a batch reactor and in a fixed-bed column. The adsorption equilibrium and kinetics had been studied by batch adsorption experiments. Equilibrium parameters and protein diffusivities were estimated by matching the models with the experimental data. Using the parameters of equilibrium and kinetics, various models, such as axial diffusion model, linear driving force model, and constant pattern model, were used to simulate the breakthrough curves on the columns. As a result, the most suitable isotherm was the Langmuir–Freundlich model, and the ionic strength had no effect on the adsorption capacity of chelate media. In addition, the pore diffusion model fitted very well to the kinetic data. The pore diffusivities decreased with increasing the initial protein concentration, however had little change with the ionic strength. The results also indicated that the models predict breakthrough curves reasonably well to the experimental data, especially at low initial protein concentration (0.3 mg ml^{-1}) and low flow rate (34 cm h^{-1}). By the results, we optimized the experimental conditions of a chromatographic process using immobilized metal affinity chromatography to purify recombinant human-like collagen.

Keywords Recombinant human-like collagen · Breakthrough curves · Immobilized metal affinity chromatography · Kinetics · Optimize

X.-J. Wang · D.-D. Fan (✉) · Y.-E. Luo
Department of Chemical Engineering, Northwest University, Xi'an 710068, China
e-mail: fandaidi@nwu.edu.cn

X.-J. Wang
Department of Environmental and Chemical Engineering, Xi'an Polytechnic University, Xi'an 710048, China

D.-D. Fan
Key Laboratory of Resource Biology and Biotechnology in Western China, Northwest University, Ministry of Education, Xi'an 710068, China

Humana Press

Nomenclature

a Specific surface area of particle (m^2/m)
C Protein concentration in bulk fluid phase (mg/ml)
C_0 Initial protein concentration in bulk fluid phase (mg/ml)
C^* Equilibrium concentration in bulk fluid phase (mg/ml)
C_p Protein concentration in pore (mg/ml)
D_e Effective diffusivity (m^2/s)
D_0 Molecular diffusivity in free solution (m^2/s)
D_p Pore diffusivity (m^2/s)
D_z Axial dispersion coefficient (m^2/s)
F Volumetric ratio of solid phase to liquid phase
K_b Association constant in Langmuir isotherm
k Constant in Freundlich isotherm
K_f Total transfer coefficient (m/s)
k_f Liquid film mass transfer coefficient on the particle surface (m/s)
L Column length (m)
Mr Molecular weight (kDa)
n Constant in Freundlich isotherm
q_* Adsorbed protein density (mg/ml)
q_0 q in equilibrium with C_0 (mg/ml)
q_m Adsorption capacity in Langmuir isotherm (mg/ml)
$\overline{q}$ Adsorbent particle average concentration (mg/ml)
R Mean particle radius (m)
r_g Radius of gyration of proteins (m)
T Temperature (K)
t Time (min)
u Interstitial velocity (cm/h)
V_b Bed volume (ml)
V_L Volume of solution (ml)
V_S Volume of wet gel (ml)
V_v Bed void volume (ml)
ε_c Column void fraction
ε_p Effective intraparticle porosity for protein
ρ Liquid phase density (kg/m^2)
μ_L Viscosity of feed solution (Pa·s)

Introduction

Collagen accounts for up to 75% of the weight of the dermis and is responsible for the resilience and elasticity of the skin [1]. Collagen is widely used as medicine, food, and chemicals. More than 50,000 tons of collagen are used in medical applications annually. Collagen is normally extracted from animal tissues, but the process is expensive and laborious and may be contaminated with viruses, and prions existed in animal tissues. Many scientists have reported to produce virus-free collagen using tobacco, silkworms, and recombinant yeast; however, the collagen productivity in these preparations was too low to bring to industrialization [2].

Recombinant human-like collagen was expressed in *Escherichia coli* BL21 using a modified human collagen complementary DNA fragment with a 6× histidine epitope

attached to the C terminus of protein [3]. Besides the close molecular weight (90 kDa), human-like collagen also contains a tri-helix structure similar to the type I collagen. However, unlike one α_1- and two α_2-chains in type I collagen structure, human-like collagen comprises three identical modified α-chains. The immunogenicity of recombinant human-like collagen is low compared with collagen isolated from animal tissues by conventional extraction methods [3–5] and has the added advantage of being free of viruses and prions.

Immobilized metal-chelate affinity chromatography has proven to be a powerful tool in the purification of histidine-tagged recombinant proteins [6–7]. A number of amino acid residues contribute to binding of proteins to chelated metal ions, but histidine residues are known to form particularly strong complexes with Cu^{2+}, Zn^{2+}, Ni^{2+}, and Co^{2+} [8]. Therefore, histidine-tagged affinity chromatography is most frequently used for the purification of recombinant proteins. Immobilized metal affinity chromatography (IMAC) is mostly used as an effective method for the capture of histidine-tagged proteins from complex protein mixtures [9–10].

Kinetics model plays important roles in technology transferring from laboratory scale to industrial scale. Appropriate models can help analyze and explain experimental data, identify process mechanisms, predict answers to operational conditions changing, and optimize processes [11]. In recent years, many mathematical models have been tested to represent the biosorption of different proteins in fixed-bed columns. The dynamics of adsorption in a fixed-bed column can be described by means of a model based on the differential mass balances of the components for the liquid and solid phases and the mass transfer from liquid to sorbent [12].

The aim of the present work was to model recombinant human-like collagen in an IMAC fixed-bed column. By the study on adsorb equilibrium and dynamics, the breakthrough curves and parameters of models were determined. According to the kinetics results, we optimized operational conditions on IMAC column for purification of recombinant human-like collagen.

Materials and Methods

Materials

Affinity chromatography media, Matrex Cellufine Chelate, was obtained from Millipore. All other reagents were of analytical grade.

Recombinant Human-Like Collagen A plasmid containing a kanamycin resistance gene that allowed temperature induction was constructed in our lab [3]. Batch and fed-batch cultivations were carried out in an in situ autoclaved fermentor to achieve high-level expression of the target protein [5]. The cells were harvested with centrifuge at 6,000×*g* for 30 min. Cell biomass (20 g) was suspended in 5 mM Tris buffer, pH 8.0 (120 ml) containing 1 mM EDTA and homogenized by sonication on ice. Cell debris was removed by centrifugation at 10,000×*g* 4°C for 30 min. The supernatant was gradient-precipitated by ammonium sulfate. The sediments from 15% to 65% (saturation degree of ammonium sulfate) were collected and dissolved in 20 mmol l^{-1} Tris buffer, pH 8.0. The affinity media, to which iminodiacetic acid (IDA) had been immobilized, was bounded with Cu^{2+}. Then, the protein was purified by IDA-Cu^{2+} resin using IMAC [13].

Determination of Effective Intraparticle Porosity (ε_p)

The effective intraparticle porosity of the chelate media for recombinant human-like collagen was determined using a batch diffusion technique [14]. Protein was buffered in 0.01 M phosphate buffer, pH 4.0, with 1.0 M sodium chloride. About 1–2 g chelate media (wet mass) pre-equilibrated in the buffer was added to flasks each containing 10 ml (V_L) of the buffered protein solution of a definite concentration. The flasks were incubated for 10 h in the shaking incubator at 160 rpm, 20°C to allow partitioning equilibrium to be reached. It was confirmed that the proteins was not adsorbed to the media under this condition [13]. Then, the liquid phase protein concentrations were determined with the UV–vis spectrophotometer at 280 nm, and the effective intraparticle porosity of the chelate media is calculated by:

$$\varepsilon_p = \frac{V_L}{V_S}\left(\frac{C_0 - C}{C}\right) \tag{1}$$

where V_S is volume of the wet gel used.

Triplicate experiments were carried out at initial recombinant human-like collagen concentrations (C_0) of 0.5, 1.0, and 2.0 mg/ml, respectively, and the effective intraparticle porosity values thus obtained were averaged and the standard deviations determined.

Determination of Column Void Fraction (ε_c)

The column void fraction, ε_c, was determined by the measure of the void volume (volume of distilled water required to fill the bed) [15]. The column was filled with chelate media, and distilled water was added to fill completely the bed. The water was then trained from the bottom of the column using a minimum period of 24 h. Afterwards, a peristaltic pump fed the column from a reservoir that contained a defined volume of distilled water. The necessary volume of water to fill the bed was determined initially by the difference between the volume contained in the reservoir and the volume remaining after filling the bed. The column void fraction was calculated using the following equation:

$$\varepsilon_c = \frac{V_v}{V_b} \tag{2}$$

where V_v is the bed void volume and V_b the bed volume.

Sorption Equilibrium Experiments

Batch equilibrium sorption experiments [16] were carried out in 50-ml Erlenmeyer flasks, containing 10 ml of the buffered protein solutions (initial concentration range from 0.1 to 1 mg/ml), into which 0.05 g of dry chelate media was added. The suspensions were agitated on a rotary shaker at 160 rpm. After 12 h, the sorption equilibrium was reached; the solution was separated by vacuum filtration and analyzed by a spectrophotometer at 280 nm.

The equilibrium concentration of protein in the solid phase (q^*) was calculated from the initial concentration (C_0) and the equilibrium concentration (C^*), in each flask, using the following equation:

$$q^* = \frac{V_L\left(C_0 - C^*\right)}{V_s}. \tag{3}$$

All equilibrium sorption experiments were carried out in duplicate.

Adsorption Kinetics Experiments

Adsorption kinetics was performed in the phosphate buffer using the stirring batch adsorption method. Dry chelate media (0.05 g) were added into ten 50-ml Erlenmeyer flasks, each containing 10 ml of the buffered protein solutions of the same initial concentration, and agitated on a rotary shaker at 160 rpm. The flasks were taken out successively from the shaker for supernatant measurement; about 5 ml of the liquid in the flask was pumped out of the flask through a 2-μm stainless filter to determine the protein concentration by a spectrophotometer at 280 nm. By this procedure, the time course of the liquid phase concentration decrease was determined.

Continuous-Flow Sorption Column System

Continuous-flow sorption experiments were conducted in a glass column with the controlled temperature. The column's height and diameter were 30 and 1.5 cm, respectively. A peristaltic pump was used to feed protein solution to the column at a stable flow rate. Liquid samples of the concentration of recombinant human-like collagen were collected at predefined time intervals. When the system reaches equilibrium, the protein concentration in the fluid phase was constant along the column and equal to the feed concentration ($C = C_0$). The temperature of stream feeding solution and of the column was controlled at 20°C through a thermostatic bath.

Mathematical Model

Sorption Equilibrium Isotherms

There are many experimental biosorption equilibrium isotherms. The main widely accepted models for single solute systems are the Langmuir, Freundlich, and Langmuir–Freundlich isotherms, described by Eqs. 4, 5, and 6, respectively:

$$q = \frac{q_{\mathrm{m}} K_{\mathrm{b}} C}{1 + K_{\mathrm{b}} C} \tag{4}$$

where q_{m} and K_{b} are the Langmuir constants.

$$q = kC^n \tag{5}$$

where k and n are the Freundlich constants.

$$q = \frac{q_{\mathrm{m}} K_{\mathrm{b}} C^n}{1 + K_{\mathrm{b}} C^n}. \tag{6}$$

In this experiment, the three isotherms were compared, and the most suitable one was determined.

Pore Diffusion Model

In this experiment, the adsorption kinetics of recombinant human-like collagen is analyzed by pore diffusion model. The model is constructed on the basis of the following assumptions [16]: The adsorbent particles are spherical, with uniform size and density, and

the functional groups of the adsorption are evenly distributed throughout the interior surface of the particle. The void fraction of the adsorption for a protein is constant during the adsorption process. Adsorption equilibrium can be represented by the suitable isotherm.

This model assumes that the driving force for intraparticle mass transfer is protein concentration gradient in the pore phase, and the protein adsorbed to the available binding sites in the pore walls remains fixed and there is no surface diffusion. The governing continuity equation for the intraparticle mass transfer by pore diffusion is described as follows:

$$\varepsilon_{\mathrm{p}} \frac{\partial C_{\mathrm{p}}}{\partial t} + \frac{\partial q}{\partial t} = \frac{\varepsilon_{\mathrm{p}} D_{\mathrm{p}}}{r^2} \frac{\partial}{\partial r} \left(r^2 \frac{\partial C_{\mathrm{p}}}{\partial r} \right) \tag{7}$$

where D_{p} is the pore diffusivity in the pore diffusion model.

$$D_{\mathrm{e}} = \varepsilon_{\mathrm{p}} D_{\mathrm{p}} \tag{8}$$

where D_{e} is the effective pore diffusivity.

In the batch adsorption system described above, the mass transfer of protein from the liquid phase to the solid phase is expressed by:

$$\frac{dC}{dt} = -\frac{3F\varepsilon_p D_p}{R} \left(C - C_p \big|_{r=R} \right) \tag{9}$$

where F is the volumetric ratio of solid phase to liquid phase.

$$F = \frac{1 - \varepsilon_{\mathrm{c}}}{\varepsilon_{\mathrm{c}}} \tag{10}$$

where ε_{c} is void fraction.

The initial and boundary conditions for Eqs. 7 and 9 are as follows:

$$\mathrm{IC}: t = 0, q = 0, C_p = 0, C = C_0 \tag{11a}$$

$$\mathrm{BC1}: r = R, C_{\mathrm{p}} = C \tag{11b}$$

$$\mathrm{BC2}: r = 0, \frac{\partial C_{\mathrm{p}}}{\partial r} = 0 \tag{11c}$$

Equation 11b holds when the external liquid-film mass transfer resistance is negligible.

Axial Diffusion and Linear Driving Force Model

The prediction of breakthrough curve is the basic of design and operation in fixed-bed adsorption. Axial diffusion model can be applied to predict the breakthrough curve in continuous-flow sorption column. The model is constructed on the basis of the following assumptions [17]: Both the mobile and stationary phases are distributed throughout the column in the same manner. An infinitesimally small control volume anywhere in the column will typify the functioning of the entire column. The flow through a packed column is a steady plug flow; with this assumption, the mobile-phase velocity is taken to be a constant that does not depend on time or radial position. Properties such as solute diffusion coefficients are also constants throughout the column.

The basic equation of the model is described as [18]:

$$\frac{\partial C}{\partial t} = D_z \frac{\partial^2 C}{\partial z^2} - u\frac{\partial C}{\partial z} - \frac{1-\varepsilon_c}{\varepsilon_c}\frac{\partial q}{\partial t} \tag{12}$$

where u is interstitial velocity and D_z is axial dispersion coefficient.

The axial dispersion coefficient is calculated with Chung correlations [19]:

$$D_z = \frac{\varepsilon_c u L}{0.2 + 0.11\,\mathrm{Re}^{0.48}} \tag{13}$$

where $\mathrm{Re} = 2Ru\rho/\mu_L$.

The initial and boundary conditions for Eq. 12 are as follows:

$$\mathrm{IC}: C = 0, t = 0 \tag{14a}$$

$$\mathrm{BC1}: C = C_0 + \frac{D_z}{u}\left.\frac{\partial C}{\partial z}\right|_{z=0}, t > 0, z = 0 \tag{14b}$$

$$\mathrm{BC2}: \frac{\partial c}{\partial t} = 0, t > 0, z = L. \tag{14c}$$

When both considered external liquid-film mass transfer resistance and intraparticle mass transfer, the linear driving force equation is expressed by [18]:

$$\frac{\partial \overline{q}}{\partial t} = K_f a\left(C - C^*\right). \tag{15}$$

K_f can correspond with other parameters obtained from the other different approximate models. In this model, K_f is the total transfer coefficient, a is the specific area of the particles, and C^* is the fluid concentration in equilibrium with the solid-phase concentration.

The parameter for Eq. 15 is calculated as follows [20]:

$$k_f a = \left(\frac{R^2}{15D_e} + \frac{R}{3k_f}\right)^{-1} \tag{16}$$

$$k_f = 1.15u(\varepsilon_c \mathrm{Re})^{-1/2} Sc^{-2/3} \tag{17}$$

where $Re = 2Ru\rho/\mu_L$., $Sc = \mu_L/\rho D_0$

The correlation of D_0 is as follows [21]:

$$D_0 = 6.85 \times 10^{-12}\frac{T}{\mu_L\left(M_r^{1/3} r_g\right)^{1/2}}. \tag{18}$$

Constant Pattern Model

The constant pattern model assumes that the concentration profiles in the stationary and mobile phases move through the column as a constant pattern or wave [17].

In affinity chromatography, adsorption columns can be operated in binding-elution cycles. To model what occurs inside the column and at the column exit, the constant pattern model separates the binding cycle to five steps. In step I, shortly after starting the binding cycle, q reaches its maximum value q_0^* in the zone near the column entrance. Thus, the entrance of the column contains a stationary phase that is saturated with protein; it can no longer remove protein from the mobile phase. The mobile phase near the column entrance is at its maximum concentration C_0 as well. During this part of the binding cycle, the concentration of protein exiting the column is essentially zero. In step II, the profiles of q and C develop into consistent patterns that move down the column with time. During step II, the column exit concentration is still essentially zero. The most important development in the binding cycle comes in step III, when the leading edge of the q and C profile reach the column exit. At this point, a breakthrough of protein occurs—the column exit concentration of protein starts to climb. In step IV, the change in the column exit concentration with time can be recorded. Finally, in step V, the column is fully saturated. Thus, the column exit concentration equals the feed concentration.

Constant patterns in both q and C suggest that directly behind the wave [17]:

$$\frac{q}{C} = \left(\frac{q}{C}\right)_{\text{equilibrium}} = \frac{q_0^*}{C_0} \tag{19}$$

where $q_0^* = \frac{q_m K_b C_0^n}{1+K_b C_0^n}$.

The assumption of constant patterns leads to a simple equation relating the stationary- and mobile-phase concentrations.

Results and Discussion

Adsorption Isotherms

The experimental results of the equilibrium study were presented in Fig. 1 and Table 1. It was shown that the experimental data were best fitted with Langmuir–Freundlich isotherm

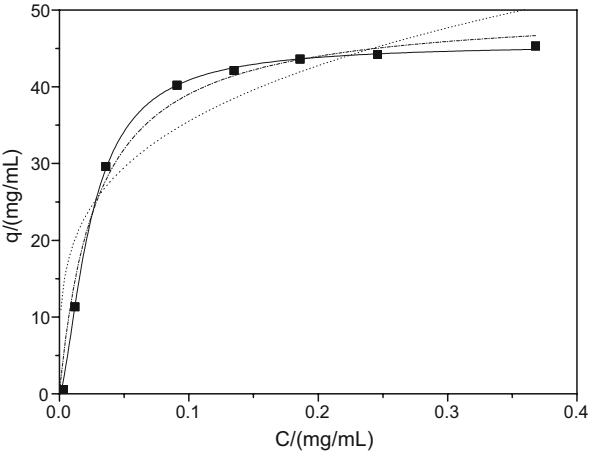

Fig. 1 Static adsorption isotherms of recombinant human-like collagen on the chelate media. The *solid line* is calculated with the Langmuir–Freundlich equation, the *dotted line* is calculated with the Freundlich equation, and the *dashed line* is calculated with the Langmuir equation

Table 1 Comparison of three kinds of isotherms.

C (mg/ml)		0.012	0.091	0.186	0.368
q (mg/mL) experimental		11.3	40.2	43.6	45.3
Langmuir model	*q* (mg/ml)	15.02	38.2	43.54	46.67
	Deviation (%)	32.92	4.98	1.38	3.02
Freundlich model	*q* (mg/ml)	20.23	34.61	41.91	50.33
	Deviation(%)	79.03	13.91	3.88	11.1
Langmuir–Freundlich model	*q* (mg/ml)	11.78	40.23	43.64	44.88
	Deviation (%)	4.25	0.07	0.09	0.93

(Eq. 6). The Freundlich isotherm is an empirical equation. The Langmuir isotherm is a homogeneous model based on the theoretical principle that only a single adsorption layer exists on an adsorbent. Langmuir–Freundlich isotherm, on the other hand, is a heterogeneous model [22]. Recombinant human-like collagen is heterogeneous material containing binding sites with a wide array of binding affinities and selectivities. So the binding behavior of IDA-Cu^{2+} resin and recombinant human-like collagen can be accurately modeled by the Langmuir–Freundlich isotherm. Therefore, in this experiment, the Langmuir–Freundlich isotherm was used in the following kinetics model calculations.

In general, the equilibrium constants q_m, K_b, and n are influenced by ionic strength. The values of equilibrium constants differ in different sodium chloride concentrations of buffer. The results were shown in Fig. 2, and the equilibrium constants in different ionic strengths were shown in Table 2. The results indicated that the adsorption capacity of chelate media to recombinant human-like collagen had little change when the ionic strength was increased. It is largely because the chelate metal ion and recombinant human-like collagen are linked with distribution bond which is influenced little by ionic strength.

Adsorption Kinetics

Experiments were performed to determine the uptake rate of recombinant human-like collagen on chelate media. Equations 7 and 9, together with the boundary conditions, were

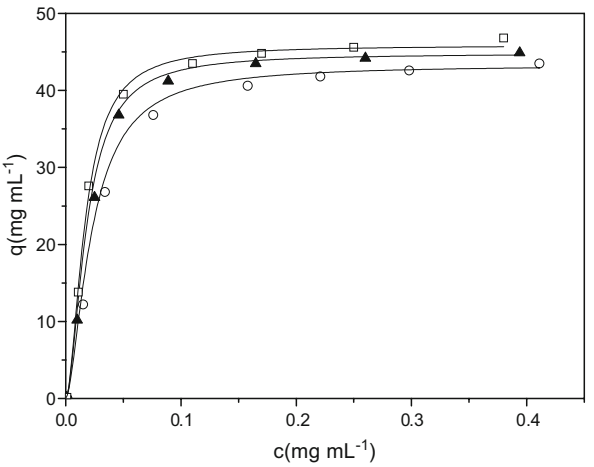

Fig. 2 Examples of experimental and simulated sorption isotherms in different ionic strength. *Solid lines* are calculated from the Langmuir–Freundlich equation. The ionic strength are (*circle*) 0.1, (*triangle*)0.5, (*square*) 0.8 mol l^{-1}

Table 2 Parameters in different ionic strength and coefficients of determination of the PDM.

I (mol l^{-1})	q_m (mg ml^{-1})	K_b ($\times 10^5$)	Number	D_p ($\times 10^{-11}$ m^2 s^{-1})	D_e ($\times 10^{-12}$ m^2 s^{-1})	R^2
0.1	43.80	0.61	1.64	2.83	6.79	0.9712
0.5	45.24	1.32	1.75	2.86	6.86	0.9921
0.8	45.84	1.48	1.79	2.85	6.84	0.9727

solved numerically by the orthogonal collocation method [23] to predict the change in liquid-phase protein concentration versus time, and the simulation results were fitted to the dynamic adsorption profile to determine the pore diffusivities of recombinant human-like collagen to chelate media by the method of Zhang and Sun [14]. Figures 3 and 4 showed that the pore diffusion model (PDM) predicted the dynamic adsorption profiles very well.

It was found that the pore diffusivities for human-like collagen decreased with increasing the initial protein concentration, and the decreasing rate of pore diffusivities was faster at lower initial concentration as shown in Fig. 3 and Table 3. One reason is the increase of hindrance effect caused by the adsorption of protein. The pore size would become small upon protein adsorption, and higher initial protein concentration would result in higher protein adsorption density, leading to more significant decrease of the pore size near the adsorbent surface. When the adsorption became saturated at high initial concentrations, further increase of the initial concentration would not create additional decrease of the pore diffusivity. The other reason is the increase in solution viscosity with increasing the collagen concentration.

The uptake curves of recombinant human-like collagen to chelate media at different ionic strengths were exhibited in Fig. 4. The best fitting values of the effective pore diffusivity (D_e) values thus obtained for recombinant human-like collagen were given in Table 2. From Table 2 and Fig. 2, it could be observed that the adsorption capacity did not change with the increased ionic strength. In this case, we can conclude that there is no a great effect of the ionic strength on pore diffusivity. This conclusion is consistent with the results in Fig. 4. The shape of the kinetics curves presented little modification when the ionic strength varied. It demonstrated that the ionic strength has little influence on binding capacity of chelate media to recombinant human-like collagen. These studies reveal that it

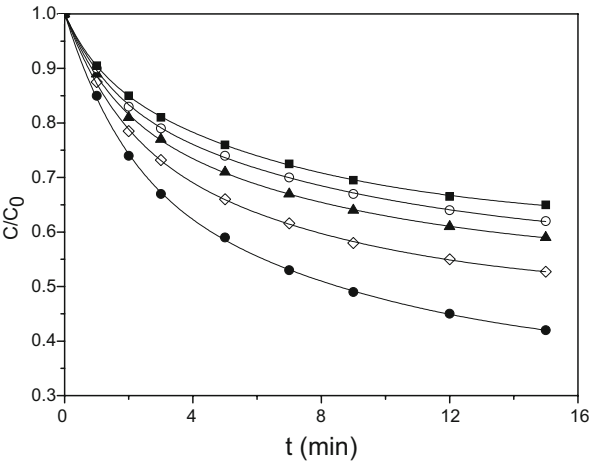

Fig. 3 Examples of experimental and simulated uptake curves of recombinant human-like collagen in different initial concentrations. *Solid lines* are calculated from the pore diffusion model. The initial concentrations of recombinant human-like collagen are (*filled circle*) 0.3, (*diamond*) 0.5, (*triangle*) 1.0, (*open circle*) 1.4, (*square*) 1.8 mg ml^{-1}

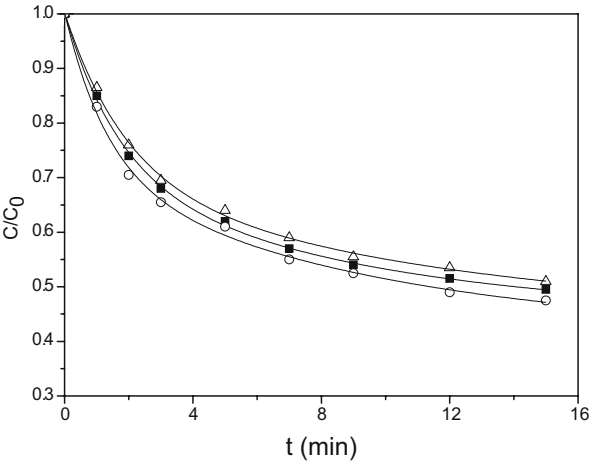

Fig. 4 Examples of experimental and simulated uptake curves of recombinant human-like collagen in different ionic strength. *Solid lines* are calculated from the pore diffusion model. The ionic strength are (*circle*) 0.1, (*filled square*) 0.5, (*open square*) 0.8 mol l^{-1}

is not electrostatic interactions which play a main role in the retention of recombinant human-like collagen on IDA-Cu^{2+} resins. The principle of the interactions lies in the metal ions acting as Lewis acids and the histidine on the protein acting as Lewis bases. These interactions are nonionic in nature and are therefore stable in high ionic strength [24].

Other parameters needed in the simulations were calculated using equations or correlations described above, which were listed in Table 4.

Simulation of Breakthrough Curves

Using independently determined model parameters, the pore diffusion model, axial diffusion model, linear driving force model, and constant pattern model were used to simulate the breakthrough curves of recombinant human-like collagen on the columns.

By Eq. 19, it can be concluded that:

$$q = \frac{q_0^*}{C_0} C = \frac{q_m K_b C^{*n}}{1 + K_b C^{*n}} \tag{20}$$

$$C^* = \left[\frac{C_0^{*(n-1)} C}{1 + K_b C_0^n - K_b C_0^{n-1} C} \right]^{1/n}. \tag{21}$$

Table 3 Parameters in different initial concentrations and coefficients of determination of the PDM.

C_0 (mg ml^{-1})	D_p ($\times 10^{-11}$ m^2 s^{-1})	D_e ($\times 10^{-12}$ m^2 s^{-1})	$K_f a$ (min^{-1})	R^2
0.3	2.85	6.84	1.10	0.9956
0.5	2.31	5.54	0.95	0.9862
1.0	2.02	4.85	0.87	0.9938
1.4	1.97	4.73	0.85	0.9967
1.8	1.83	4.39	0.81	0.9876

Table 4 Parameter values used in the models.

Parameters	ε_p	ε_c	L (cm)	R (μm)	D_0 ($m^2\ s^{-1}$)	k_f ($m^2\ s^{-1}$)
Value	0.24	0.32	20	75	2.473×10^{-11}	6.59×10^{-7}

Equation 15 can be rearranged to be:

$$\frac{\partial \overline{q}}{\partial t} = K_f a\left\{C - \left[\frac{C_0^{*(n-1)}C}{1 + K_b C_0^n - K_b C_0^{n-1} C}\right]^{1/n}\right\}. \tag{22}$$

Then, Eq. 12 can be described as:

$$\frac{\partial C}{\partial t} = D_z\frac{\partial^2 C}{\partial z^2} - u\frac{\partial C}{\partial z} - \frac{1-\varepsilon_c}{\varepsilon_c}K_f a\left\{C - \left[\frac{C_0^{*(n-1)}C}{1 + K_b C_0^n - K_b C_0^{n-1} C}\right]^{1/n}\right\}. \tag{23}$$

With Eq. 23, the initial and boundary conditions in Eqs. 14a, 14b, 14c and the independently determined model parameters listed in Table 4, we predicted and compared the breakthrough curves with the experimental data. The simulation results under different experimental conditions were plotted in Figs. 5 and 6. The model's statistical analysis was presented in Table 5. The results showed that the model predicted breakthrough curve very well. However, all the simulated breakthrough curves contained a tailing, which the models could not predict. This phenomenon may result from the extra-column effects as well as the particle size distributions [25]. Displacement of impurities or protein dimmers may also play a role when adsorption is close to equilibrium. Moreover, according to Yang and Etzel [26], the spreading of non-spherical protein will cause the asymmetry of breakthrough curves. Recombinant human-like collagen is a non-spherical molecule, so the spreading may also contribute to the asymmetry of the breakthrough curves. In addition, it is worth

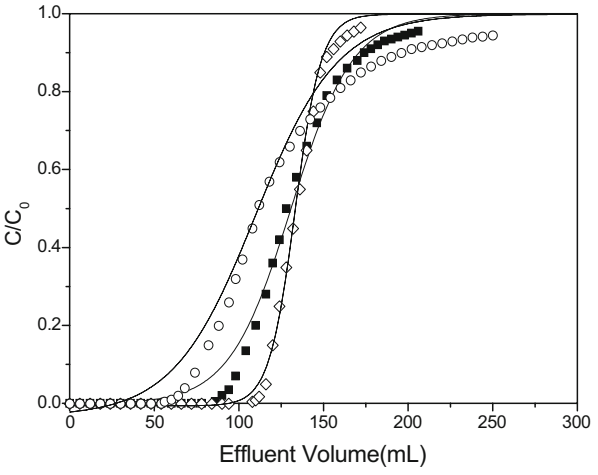

Fig. 5 Simulated and experimental recombinant human-like collagen breakthrough curves in the fixed-bed packed with the metal chelate media at the superficial velocities of (*diamond*) 34, (*square*) 102 and (*circle*) 170 cm h^{-1} at C_0=0.3 mg ml^{-1}. The *solid lines* are predicted using models

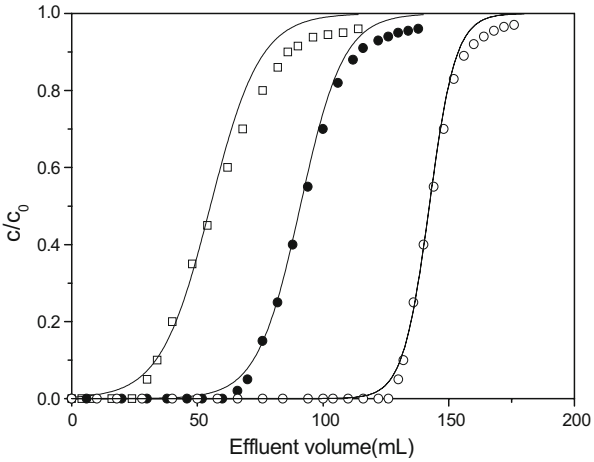

Fig. 6 Simulated and experimental recombinant human-like collagen breakthrough curves in the fixed-bed packed with the metal chelate media at the superficial flow rate of 34 cm/h. C_0=0.3 mg ml^{-1} (*open circle*); C_0=0.5 mg ml^{-1} (*filled circle*); C_0=1.0 mg ml^{-1} (*square*). The *solid lines* are predicted using models

mentioning that the model calculations were carried out using all the unadjustable parameters obtained by independent experiments or calculated from correlations. The parameters calculated from correlations might not be accurate enough for the system, which would lead to the deviations of the model predictions.

In Fig. 5, the breakthrough curves under different flow rates were simulated. It could be observed that the breakthrough curve was simulated better when the flow rate was slower. This conclusion was confirmed by the model's statistical analysis presented in Table 5. The main reason is that the contact time of stationary- and mobile-phase decreased with increasing the flow rate. In order to carry out effective adsorption, sufficient contact time must be made. When the flow rate was so fast, the protein could not spread to the internal resin adsorption. Then, the adsorption equilibrium could not be achieved. The models and experimental data would produce a certain deviation.

The simulated breakthrough curves for different feed concentrations were shown in Fig. 6. The results demonstrated that the models tested fitted the experimental results for all initial concentrations, but the breakthrough curve was sharper at lower initial concentration. The reason is that the effective pore diffusivity decreased with the increased initial concentration, as shown in Table 3.

Table 5 Coefficients of determination of the models for the simulation of the breakthrough curves.

C (mg ml^{-1})	V (cm h^{-1})	R^2
0.3	170	0.8564
0.3	102	0.9201
0.3	34	0.9875
0.5	34	0.9645
1.0	34	0.9458

Conclusions

In this article, mathematical models for flow through chromatography have been tested for a column packed with chelate media to adsorb recombinant human-like collagen. The main results obtained can be summarized as follows:

(a) The Langmuir, Freundlich, and Langmuir–Freundlich isotherms were compared. The maximum deviation of Langmuir–Freundlich isotherm (4.25%) was around 87.1% lower than Langmuir isotherm (32.92%) and 94.6% lower than Freundlich isotherm (79.03%). So the most suitable one was the Langmuir–Freundlich isotherm.
(b) The adsorption capacity of chelate media to recombinant human-like collagen had little change with increasing the ionic strength.
(c) The pore diffusion model predicted the adsorption kinetics very well. Coefficients of determination of PDM in different conditions were all more than 0.97.
(d) The pore diffusivities for recombinant human-like collagen decreased with increasing the initial protein concentration, but had little change with increasing the ionic strength.
(e) The breakthrough curve was simulated better when the flow rate was slower. The simulated breakthrough curves fitted the experimental results for all initial concentrations, but the breakthrough curve was sharper at lower initial concentration.

These results have important general implications for the design, optimization, and scale-up of a chromatographic process using IMAC to purify recombinant human-like collagen. By the kinetics results, we optimized the experimental conditions. A column with Cu^{2+}-IDA chelate media was equilibrated with phosphate buffer (pH 7.0, 500 mmol l^{-1} NaCl). The column was loaded with the probe (initial protein concentration was 0.3 mg ml^{-1}) at a flow rate of 34 cm h^{-1} for 2.2 h and washed with ten volumes of equilibrate buffer. Bound proteins were eluted with elution buffer (0.2 mol l^{-1} phosphate buffer, pH 7.5, 1 mol l^{-1} NaCl, 1 mol l^{-1} NH_4Cl).

This work provided guidelines for designing industrial-scale separations of recombinant human-like collagen using IMAC.

Acknowledgments This work was supported by grants from the National Science and Technology Key Funds (2003DA901A32) and the National Natural Science Foundation (20476085 and 20606026).

References

1. Calleja-Agius, J., Muscat, B. Y., & Brincat, M. P. (2007). Skin ageing. *Menopause International*, *13*, 60–64. doi:10.1258/175404507780796325.
2. Olsen, D., Yang, C. L., Bodo, M., Chang, R., Leigh, S., Baez, J., et al. (2003). Recombinant collagen and gelatin for drug delivery. *Advanced Drug Delivery Reviews*, *55*, 1547–1567. doi:10.1016/j.addr.2003.08.008.
3. Fan, D. D., Duan, M. R., Mi, Y., Song, J. R., Xi, J. F., Wang, D. W., et al. (2002). High density fermentation of recombinant *E. coli* for production of human-like collagen. *Journal of Chemical Industry and Engineering (China)*, *53*, 752–754.
4. Fan, D. D., Luo, Y. E., Mi, Y., Ma, X. X., & Shang, L. A. (2005). Characteristics of fed-batch cultures of recombinant *Escherichia coli* containing human-like collagen cDNA at different specific growth rates. *Biotechnology Letters*, *27*, 865–870. doi:10.1007/s10529-005-6720-8.
5. Luo, Y. E., Fan, D. D., Ma, X. X., Wang, D. W., Mi, Y., Hua, X. F., et al. (2005). Process control for production of human-like collagen in fed-batch culture of *Escherichia coli* BL 21. *Chinese Journal of Chemical Engineering*, *13*, 276–279.

6. Dalziel, J. E., Shu, S. W., Thai, P., Yan, L. Z., & James, D. (2007). Expression of human BK ion channels in Sf9 cells, their purification using metal affinity chromatography, and functional reconstitution into planar lipid bilayers. *Journal of Chromatography. B, Analytical Technologies in the Biomedical and Life Sciences*, *857*, 315–321. doi:10.1016/j.jchromb.2007.07.033.
7. Hutchinson, M. H., & Howard, A. C. (2006). Adsorptive refolding of histidine-tagged glutathione S-transferase using metal affinity chromatography. *Journal of Chromatography. A*, *1128*, 125–132. doi:10.1016/j.chroma.2006.06.050.
8. Lavanant, H., Emilie, H., & Yannik, H. (1999). Complexes of -histidine with Fe^{2+}, Co^{2+}, Ni^{2+}, Cu^{2+}, Zn^{2+} studied by electrospray ionization mass spectrometry. *International Journal of Mass Spectrometry*, *185–187*, 11–23. doi:10.1016/S1387-3806(98)14044-7.
9. Yan, P. T., Tau, C. L., Wen, S. T., Khatijah, Y., & Beng, T. T. (2006). Recovery of histidine-tagged nucleocapsid protein of Newcastle disease virus using immobilised metal affinity chromatography. *Process Biochemistry*, *41*, 764–881. doi:10.1016/j.procbio.2005.09.011.
10. Finzi, A., Cloutier, J., & Éric, A. (2003). Two-step purification of His-tagged Nef protein in native condition using heparin and immobilized metal ion affinity chromatographies. *Journal of Virological Methods*, *111*, 69–73. doi:10.1016/S0166-0934(03)00154-X.
11. Kim, J. Y., & Cramer, M. S. (1994). Experimental studies in metal affinity displacement chromatography of proteins. *Journal of Chromatography. A*, *686*, 193–203. doi:10.1016/0021-9673(94)00685-7.
12. Ozdural, A. R., Aslı, A., & Piet, J. A. M. (2004). Modeling chromatographic columns Non-equilibrium packed-bed adsorption with non-linear adsorption isotherms. *Journal of Chromatography. A*, *1041*, 77–85. doi:10.1016/j.chroma.2004.05.009.
13. Wang, X. J., & Fan, D. D. (2005). Purification of recombinant human-like collagen by using metal chelated affinity chromatography. *Journal of chemical engineering of Chinese universities*, *19*, 410–413.
14. Zhang, S. P., & Sun, Y. (2002). Ionic Strength dependence of protein adsorption to dye-ligand adsorbents. *AIChE Journal. American Institute of Chemical Engineers*, *48*, 178–186. doi:10.1002/aic.690480118.
15. da Silva, E. A., Eneida, S. C., Celia, R. G. T., Lucio, C. F., & Reginaldo, G. (2002). Modeling of copper (II) biosorption by marine alga *Sargassum* sp. In fixed-bed column. *Process Biochemistry*, *38*, 791–799. doi:10.1016/S0032-9592(02)00231-5.
16. Chen, W. D., Dong, X. Y., & Sun, Y. (2002). Analysis of diffusion models for protein adsorption to porous anion-exchange adsorbent. *Journal of Chromatography. A*, *962*, 29–40. doi:10.1016/S0021-9673(02)00466-1.
17. Antonio, A. G., Matthew, R. B., Jaime, R. V., Mariam, S., & Anil, V. (2002). *Bioseparation process science*. Beijing: Tsinghua University Press.
18. Chen, W. D., Dong, X. Y., & Sun, Y. (2003). Dependence of pore diffusivity of protein on adsorption density in anion-exchange adsorbent. *Biochemical Engineering Journal*, *14*, 45–50. doi:10.1016/S1369-703X(02)00118-3.
19. Chung, S. F., & Wen, C. Y. (1968). Longitudinal dispersion of liquid flowing through fixed and fluidized beds. *AIChE Journal. American Institute of Chemical Engineers*, *14*, 857–866. doi:10.1002/aic.690140608.
20. Leitão, A., & Rodrigues, A. (1999). Modeling and simulation of protein adsorption in permeable chromatographic packings: a double linear driving force model. *Biochemical Engineering Journal*, *3*, 131–139. doi:10.1016/S1369-703X(99)00011-X.
21. He, L. Z., & Niemeyer, B. (2003). A novel correlation for protein diffusion coefficients based on molecular weight and radius of gyration. *Biotechnology Progress*, *19*, 544–548. doi:10.1021/bp0256059.
22. Umpleby, R. I., Baxter, S. C., Chen, Y., Shah, R. N., & Shimizu, K. D. (2001). Characterization of molecularly imprinted polymers with the Langmuir–Freundlich isotherm. *Analytical Chemistry*, *73*, 4584–4591. doi:10.1021/ac0105686.
23. He, L. Z., Dong, X. Y., & Sun, Y. (1998). A diffusion model of protein and eluant for affinity filtration. *Biochemical Engineering Journal*, *2*, 53–62. doi:10.1016/S1369-703X(98)00017-5.
24. Beasley, J. R., David, A. D., Tiffany, L. W., Susan, M. P., John, M. L., & Douglas, S. A. (2003). Evaluation of compound interference in immobilized metal ion affinity-based fluorescence polarization detection with a four million member compound collection. *Assay and Drug Development Technologies*, *1*, 455–459. doi:10.1089/154065803322163768.
25. Carta, G., & Ubiera, A. (2003). Particle-size distribution effects in batch adsorption. *AIChE Journal. American Institute of Chemical Engineers*, *49*, 3066–3073. doi:10.1002/aic.690491208.
26. Yang, H., & Etzel, M. R. (2003). Evaluation of three kinetic equations in models of protein purification using ion-exchange membranes. *Industrial & Engineering Chemistry Research*, *42*, 890–896. doi:10.1021/ie020561u.